




AKADÉMIAI KIADÓ

# Modeling of stress-strain relation of cement-treated sand under compression

Khawaja Adeel Tariq<sup>1\*</sup>  and Takeshi Maki<sup>2</sup>

Pollack Periodica •  
An International Journal  
for Engineering and  
Information Sciences

16 (2021) 3, 94–100

DOI:

[10.1556/606.2021.00322](https://doi.org/10.1556/606.2021.00322)

© 2021 Akadémiai Kiadó, Budapest

<sup>1</sup> Department of Civil Engineering, The University of Faisalabad, Faisalabad, Pakistan

<sup>2</sup> Department of Civil and Environmental Engineering, Saitama University, Saitama, Japan

Received: December 22, 2020 • Revised manuscript received: January 29, 2021 • Accepted: February 3, 2021

Published online: April 21, 2021

ORIGINAL RESEARCH  
PAPER



## ABSTRACT

This research work has been conducted to model the uniaxial stress-strain compressive behavior of cement-treated sand and its post-peak softening area. The cylindrical specimens were produced by using limestone powder, sand and high early strength cement. The mixtures were made by using different ratios of water to cement with fixed ratio of limestone powder to cement and cement to sand. The stress-strain behavior in post-peak zone of cement-treated is adjusted with introduction of compression softening factor. Uniaxial compressive stress-strain relationships after amending the Japanese Society of Civil Engineers model are proposed. Finite element analysis shows that the suggested model estimates well the compressive behavior of cement-treated sand.

## KEYWORDS

limestone, cement, sand, concrete, compressive strength

## 1. INTRODUCTION

Properties of ground soil play an important role in the design of structures supporting it. If the bearing capacity of the ground is not enough to support the superstructure load, soil improvement becomes necessary. The ground treatment depends on the type of soil. For sandy soil, cement is used to improve the foundation characteristics. The improvement can be classified into many types depending on the process involved like material selection, ground condition, structure type, etc. In most cases, the soil at the site is generally not suitable for supporting heavy loads of the superstructures. This problem can be avoided by selecting a good site or using ground improvement techniques. The ground improvement can reduce the compressibility, permeability and increases the load-carrying capacity. The strength of good quality materials depends on the purpose of use. The mix of high water content can cause bleeding. This problem can be resolved by using a non-pozzolanic filler material like limestone powder as it decreases the segregation and bleeding [1].

The soil is so far modeled on basis of plasticity theory [2, 3]. The relative displacement of small soil particles due to particle frictional resistance results in plastic deformation. Microscopic fracture in cement-treated sand may occur due to the presence of cement in soil particles. The failure of concrete structures initiates the formation of crack. The failure process of concrete involves the growth of the cracking zone with large fractures even before peak load is applied. Researchers have proposed modeling of concrete using plasticity theory for uni- and multi-axial [4]. The localized fracture of concrete specimens is used for the computation of its fracture energy subjected to tension and uniaxial compression [5]. The localized concrete fracture affects the post-peak curve in a stress-strain relationship. Deformation within the damage zone needs to estimate accurately in order to understand the post-peak softening phenomena [6]. The capacity of absorption of elastic energy reduces due to the fracture. This phenomenon is modeled by researchers as the reduction in stiffness [4].

\*Corresponding author.

E-mail: [khawajaadeel@hotmail.com](mailto:khawajaadeel@hotmail.com)

The fracture energy of the concrete also depends on the aggregate size. It increases with the increase in aggregate size used in the concrete [7].

Complex structures are modeled worldwide by researchers using the Finite Element Method (FEM) [8]. Finite element analysis was used to study the tensile strain rate effect of cementitious materials [9]. The Rayleigh damping model is used by the researcher to model the framework of FEM analysis and has successfully used it for vibration analysis of beam structures. The finite element analysis is also used by the researchers to study failure modes of the slab and bending test specimens [10, 11].

In this study, an effort has been made to investigate the uniaxial compressive stress-strain behavior of cement-treated sand. Furthermore, a model is proposed for the stress-strain relation of cement-treated sand and its softening mechanism. The applicability of the suggested model is also verified using finite element analysis.

## 2. MATERIAL AND PROCEDURES

### 2.1. Materials

The behavior of cement-treated sand was investigated by performing experiments. The test specimens were produced by using limestone powder, sand and cement (high early strength). The oven dried, poorly graded sand was used. The coefficients of curvature and uniformity of sand were 1.0 and 2.2, respectively [12]. The water absorption of sand was 1.3%. The particle densities of limestone powder, sand and cement were 2.7, 2.6 and 3.2 g/cm<sup>3</sup> respectively. The limestone powder was used as an inert filler material.

### 2.2. Mix proportions

The test variables were Water to Cement (W/C) as 100, 130, 150, 170, 190%, Limestone powder to Cement (L/C) as 130% and C/S as 30% by weight. The mix proportions used for the experiments are listed in Table 1. These ratios were finalized after trial experiments. The limestone powder was first mixed with sand; then cement was mixed. Finally water was

Table 1. Mix proportions

W/C %	Material by weight (%)			
	Water	Limestone	Sand	Cement
100	15.7	19.6	49.6	15.1
130	19.4	18.7	47.4	14.4
150	21.6	18.2	46.1	14.0
170	23.8	17.7	44.9	13.6
190	25.8	17.3	43.7	13.3

added to the mix. The specimens were cured by covering with wet cloths.

### 2.3. Testing methods

**2.3.1. Uniaxial compression test.** The strength of concrete varies with the change in height to diameter ratio. Therefore, specimens with varying height to diameter ratios (1–4) were produced. The cylindrical specimens were tested for 7 and 14 days. The internal strain distribution of test specimens was computed by using strain gauges, which were attached to a silicon bar. The tests were performed under controlled loading conditions and transducers were used to measure the average strain.

**2.3.2. Lateral cyclic load test.** Displacement controlled lateral cyclic load test was performed on a single pile. The load is applied at a height of 10 cm and cement-treated sand was cast as a 30 cm cube central block (Fig. 1). The compressive strength was 3.7 MPa. A displacement transducer was used to measure displacement at a height of 3 cm from the box surface. The dimensions of the steel box was 30 × 30 × 45 cm (length × breadth × height).

## 3. TEST RESULT AND DISCUSSION

### 3.1. Uniaxial compression test

The compressive strength development for W/C of 170% against curing period is shown in Fig. 2. Uniaxial compression test was performed for specimen having

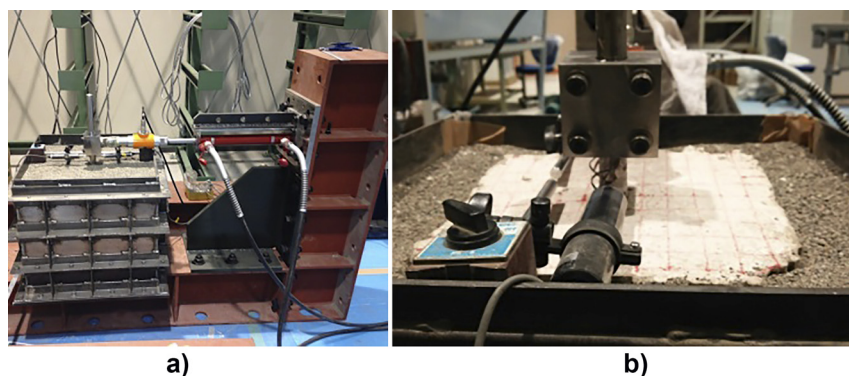


Fig. 1. a) Lateral load test setup and b) cement-treated sand casted as central part

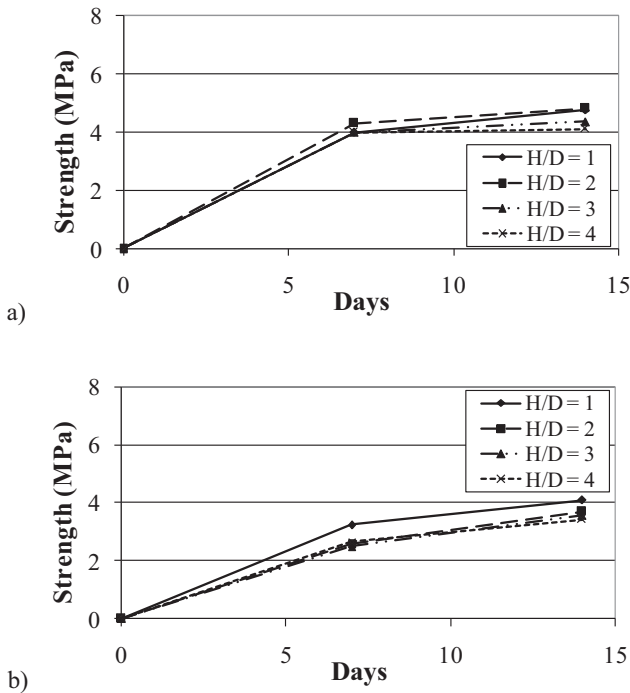


Fig. 2. Compressive strength development for specimens having W/C of 170% and diameters as a) 100 mm and b) 150 mm

varying height to diameter ratio (H/D) from 1 to 4. The results have indicated some variation in uniaxial compressive strength with the increase of specimen diameter. The cement-treated specimens were produced without using coarse aggregates. The variation in strength of cement-treated sand is not significant as presence of coarse aggregate and cement matrix affects the behavior of specimen.

### 3.2. Modeling of stress-strain relation in compression

**3.2.1. Uniaxial concrete model.** Concrete is a brittle material having nonlinear behavior at low stress state. The plasticity in concrete starts with the collapse of its fine voids. If nonlinear behavior of concrete is only explained on the basis of plasticity theory, its stiffness must remain same if plastic strain does not change. However, like any-other brittle materials, concrete stiffness during unloading is not constant. Therefore it is essential to consider nonlinear behavior. The factors that are responsible of nonlinear behavior may include formation of micro cracks and collapse of mortar and aggregates [4].

It is generally accepted that the envelope curve of concrete that provides a bond between lower and upper limit can be produced under different loading paths. The envelope curve of concrete can be studied by comparing the results of monotonic loading [13]. The nonlinear behavior of concrete due to the formation of plastic strain can be modeled by the concept of reduction in a volume of constituent material that reserves elastic strain energy. The fracture results in reducing stiffness during unloading and reloading.

The degree of the fracture can be represented by the concept of fracture parameter ( $K$ ). It is the ratio of the

constituent elements that have the capability to bear the stress. The fracture parameter has a value equal to one at the initial condition [4]. The uniaxial compressive stress-strain behavior of concrete can be estimated by using the following concrete model [14]:

$$\sigma_c = E_o K (\epsilon'_c - \epsilon'_p), \tag{1}$$

$$E_o = \frac{2f'_{cd}}{\epsilon'_{peak}}, \tag{2}$$

$$K = \exp \left\{ -0.73 \frac{\epsilon'_{max}}{\epsilon'_{peak}} \left( 1 - \exp \left( -1.25 \frac{\epsilon'_{max}}{\epsilon'_{peak}} \right) \right) \right\}, \tag{3}$$

$$\epsilon'_p = \epsilon'_{max} - 2.86 \cdot \epsilon'_{peak} \left\{ 1 - \exp \left( -0.35 \frac{\epsilon'_{max}}{\epsilon'_{peak}} \right) \right\}, \tag{4}$$

where  $\sigma_c$  is the uniaxial compressive stress;  $\epsilon'_c$  is the average axial strain;  $\epsilon'_p$  is the plastic strain;  $\epsilon'_{max}$  is the maximum strain in a loading cycle;  $E_o$  is the modulus of elasticity;  $f'_{cd}$  is the compressive strength;  $\epsilon'_{peak}$  is the peak strain;  $K$  is the fracture parameter (it is ratio of unloading stiffness,  $E_u$  to initial stiffness,  $E_o$ , Fig. 3).

The cyclic uniaxial compression test was performed in order to understand the cyclic behavior (Fig. 4). The strain

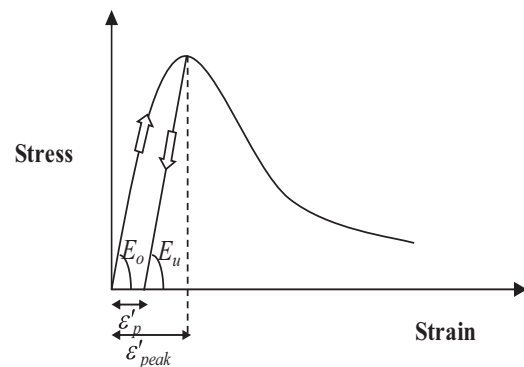


Fig. 3. Typical stress-strain curve (brittle materials)

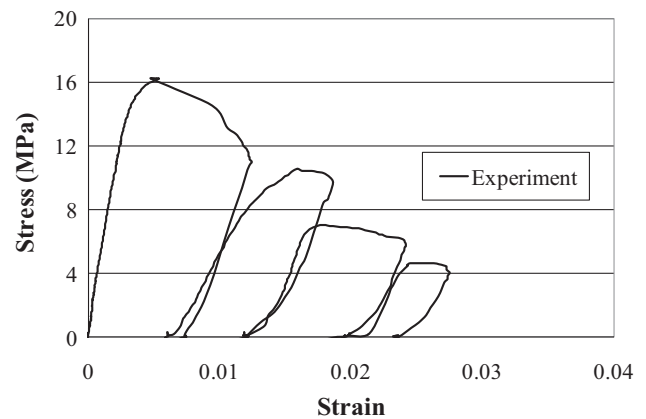


Fig. 4. Uniaxial cyclic loading test on specimens having W/C = 100% and size as on 100 x 300 mm

distributions of test specimens are also measured internally by help of strain gauges. It was observed that reduction in stiffness of cement-treated sand was not rapid as compared with brittle materials like concrete.

**3.2.2. Proposed compressive stress-strain model.** Based on the test results, the concrete model is amended for cement-treated sand. The following equations are proposed for Young’s modulus, Fracture parameter and plastic strain of cement-treated sand:

$$E_o = \frac{1.5f'_{cd}}{\epsilon'_{peak}}, \quad (5)$$

$$K = \exp\left\{-0.3 \frac{\epsilon'_{max}}{\epsilon'_{peak}} \left(1.3 - \exp\left(-1.5 \frac{\epsilon'_{max}}{\epsilon'_{peak}}\right)\right)\right\}, \quad (6)$$

$$\epsilon'_p = \epsilon'_{max} - 1.6 \cdot \epsilon'_{peak} \left\{1 - \exp\left(-0.8 \frac{\epsilon'_{max}}{\epsilon'_{peak}}\right)\right\}. \quad (7)$$

The suitability of suggested equation (Eq. 5) is shown in Fig. 5. The proposed equations within failure zone are presented graphically in Figs 6 and 7. The coefficient of determination of proposed equation in Figs 6 and 7 are about 81 and 95%, respectively.

The amended stress-strain model of cement-treated sand within failure zone is shown in Fig. 8. It is observed that proposed stress-strain equation considering amended equations of Young’s modulus, fracture parameter and plastic strain shows good agreement with experimental stress-strain behavior.

**3.2.3. Stress-strain relation dependency on element size.** The finite element analysis tools are used worldwide to model behavior of complex structures and materials. During finite element modeling, the mesh element size can be varied for structural members. If analysis at post-peak

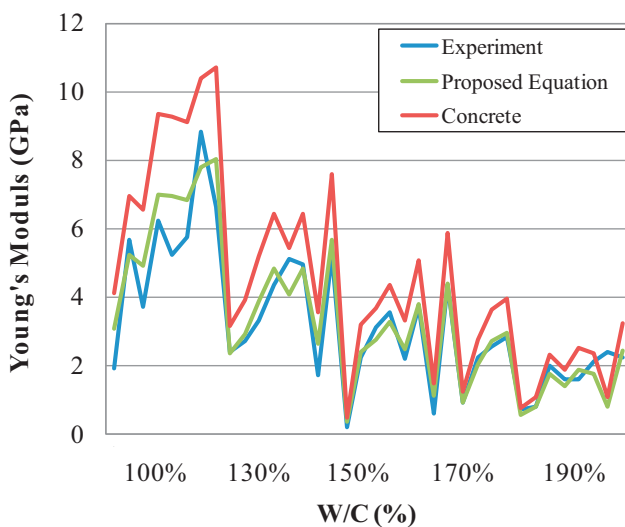


Fig. 5. Proposed equation for Young’s modulus

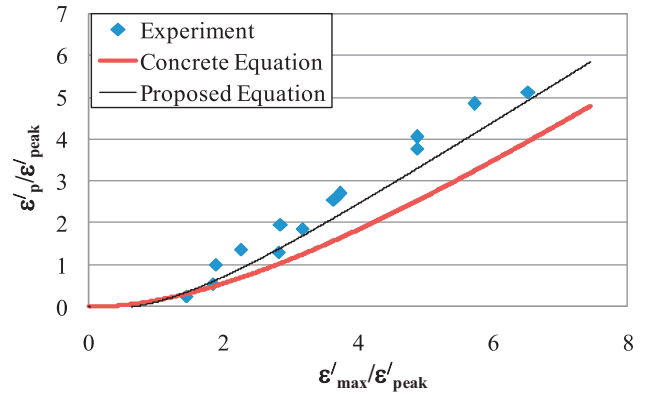


Fig. 6. Proposed equation for plastic strain ( $\epsilon'_p$ )

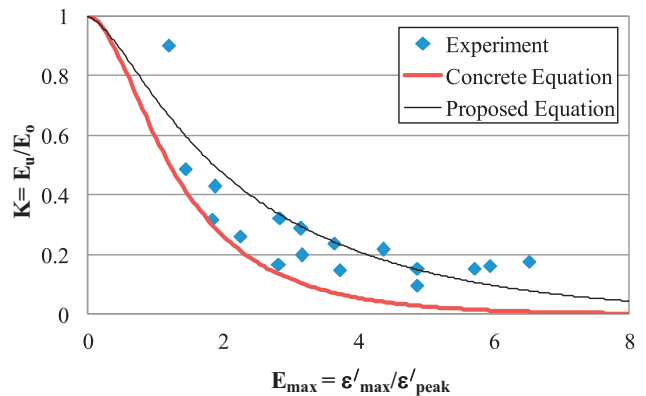


Fig. 7. Proposed equation for fracture parameter ( $K$ )

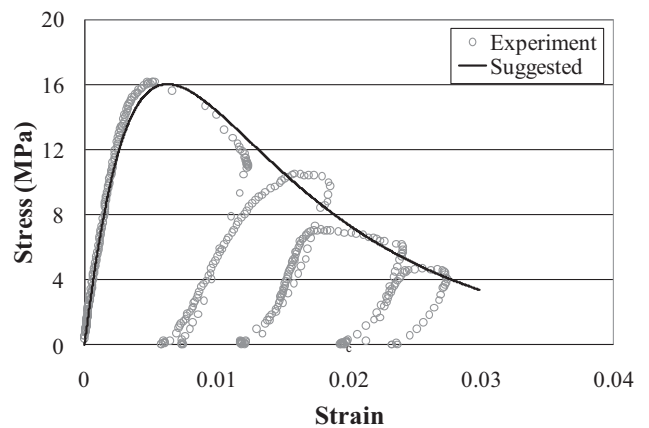


Fig. 8. Proposed equation for stress-strain

stage is required, it must be modified based on energy equilibrium and also the size of the finite element.

Constitutive model generally depends on stress-strain relationships in average state. This concept is also applied during Finite Element (FE) analysis without consideration of element size ( $L$ ). The consideration of the constant stress-strain relationship within the finite elements is not possible in reality as in large elements, localized failure zone can develop. Cement-treated sand localized compression fracture zone length ( $L_o$ ) determined from the experiment is approximately 250 mm. If

element size is below 250 mm, post-peak softening increases. It is verified through finite element analysis [15].

The post-peak stress-strain relationship of cement-treated considering element size is adjusted by the introduction of compression softening factor  $C$  (Fig. 9) based on the test results.  $C$  is a post-peak adjustment factor for the stress-strain relationship. The adjustment factor depends on  $L$  and  $L_o$ . The area under the post-peak curve is used to compute fracture energy. The stress-strain relationship obtained by using adjustment factor is shown in Fig. 10 ( $A = L/L_o = 1$ ). Concrete stress-strain equation [14] is modified for element size dependency as follows:

$$K = \exp \left\{ -0.3 \left( \frac{\epsilon'_{max}}{\epsilon'_{peak}} \right)^{(1+C)} \cdot \left( 1.3 - \exp \left( -1.5 \left( \frac{\epsilon'_{max}}{\epsilon'_{peak}} \right)^{(1+C)} \right) \right) \right\}, \tag{8}$$

where

$$C = -0.0399 \left( \frac{L}{L_o} \right)^2 + 0.6092 \left( \frac{L}{L_o} \right) - 0.5736 \tag{9}$$

and  $L_o = 250$  mm.

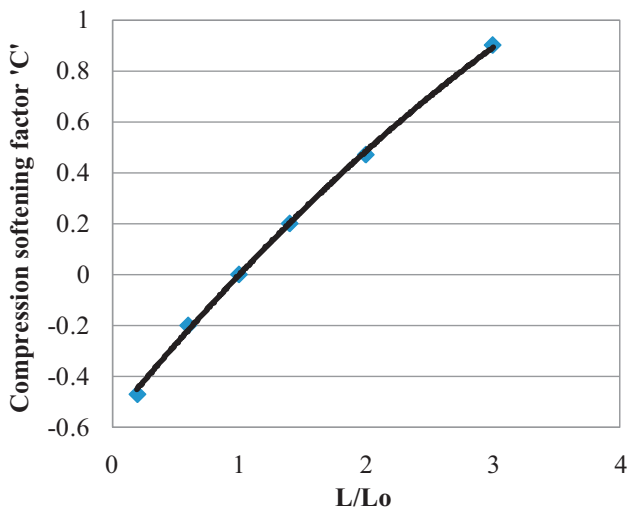


Fig. 9. Suggested compression softening factor  $C$

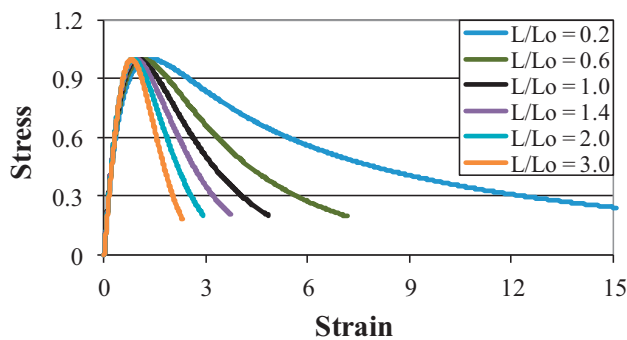


Fig. 10. Proposed post-peak stress-strain curve adjustment against ratio (symbolize as  $A$ ) of element size ( $L$ ) to fracture zone length ( $L_o$ )

### 3.3. Finite element analysis of pile

The cement-treated sand embedded single pile finite element analysis was performed. The analysis was performed for both existing and proposed model case. In proposed model case, post-peak softening curve was adjustment based on element size. During analysis, proposed model had automatically considers the element size effect.

**3.3.1. FEM model, boundary conditions and parameters.** The analysis for single steel pile having fixed bottom was carried out. The diameter and height of the pile was 2.5 and 45 cm respectively. Young's modulus, yield strength and unit weight of steel is taken as 220 GPa, 630 MPa and 7,700 kg/m<sup>3</sup> respectively. The load is applied at a height of 10 cm. The displacement transducers were attached at 3 cm from the soil surface. Marc Mentat and GID software was used for creating FEM mesh and for results visualization respectively (Fig. 11). Displacement controlled lateral cyclic load was applied. The displacement of pile was continued until it reached to 4, 10, 20, 35, 50, 75 and 100% of pile diameter. Ohsaki equation [16] is used to model sand. The finite element analysis results are compared in Fig. 12.

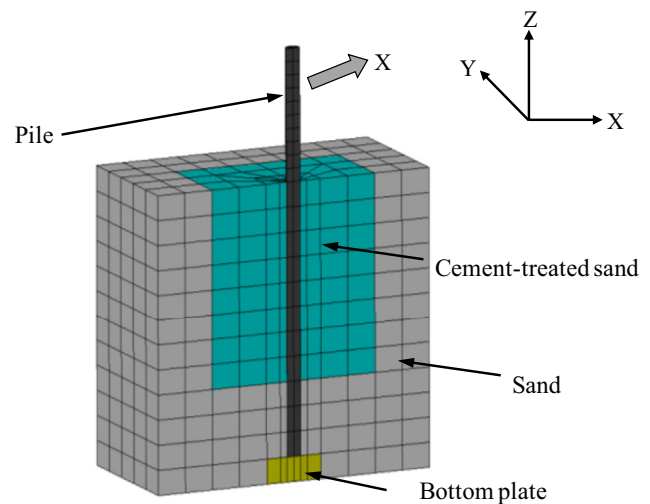


Fig. 11. FEM mesh for pile test

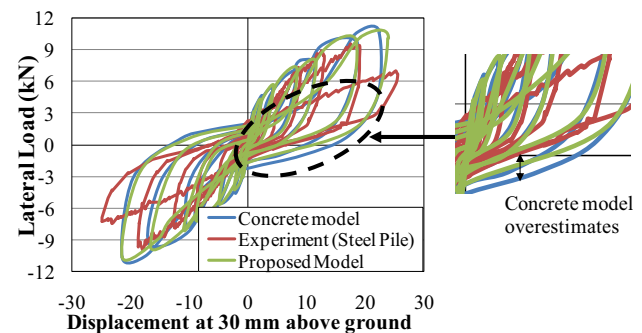


Fig. 12. Experimental result, concrete model and proposed model comparison

Table 2. Cement-treated sand and sand properties used in analysis

Analysis case*		Poisson's ratio	Young's Modulus (GPa)	Shear Modulus (GPa)	Ohsaki Coeffic.	Shear Strength (MPa)	Unit weight (kg/m <sup>3</sup> )
S+CS	S only	0.3	0.04	15.38	1.6	0.5	1,660
	CS	0.2	2.3				2,100

\*S only case (pile embedded only in sand); CS case (pile embedded in sand+ cement-treated sand, Fig. 1); Compressive strength was 3.7 MPa.

By considering the symmetry, half model analysis was carried out. Loading point, bottom plate and walls were fixed in X and Y direction. Pile and loading face was fixed in Y direction. An element (bond) was considered in between sand, cement-treated sand and pile. Bond element properties include no tensile stiffness. High compressive stiffness was also considered for bond element. The analysis case and parameters used in finite element analysis are given in Table 2.

Finite element analysis of concrete and proposed equation was performed and results are compared. It is observed from the results (Fig. 12) that the proposed equation estimates well in comparison with the concrete model.

## 4. CONCLUSIONS

The stress-strain relation of cement-treated sand under compression is modeled by help of experiments and finite element analysis. Based on the test results and finite element analysis, the following conclusions are drawn:

- The size of test specimens of cement-treated sand has negligible effect on compressive strength;
- The mechanical behavior of cement-treated sand should be modeled based on a procedure considering plasticity and fracture mechanics. The presence of cement hydrates results in microscopic fracture when cement-treated sands are subjected to load;
- The models suggested for plastic strain, fracture parameters and young's modulus estimate well the compressive behavior;
- The post-peak softening curve can be adjusted for cement-treated sand with the introduction of compression softening factor;
- FEM analysis of displacement controlled lateral load test indicates that the suggested model estimates well the post-peak softening part, whereas concrete model overestimates it;
- Further investigation is needed for accurate estimation of behavior of cement-treated sand. The research presented in this paper deals with the compressional behavior of cement-tread sand. However, in 3D environment the tensile cracking can cause reduction in compressive strength of cement-treated sand. Therefore, it needs to be clarified in future.

## ACKNOWLEDGEMENT

This research was supported by the Grant-in-Aid for Scientific Research of Ministry of Education, Culture, Sports, Science and Technology (MEXT), Japan.

## REFERENCES

- [1] H. E. Elyamany, A. E. M. Elmoaty, and B. Mohamed, "Effect of filler types on physical, mechanical and microstructure of self-compacting concrete and flow-able concrete," *Alexandria Eng. J.*, vol. 50, no. 3, pp. 295–307, 2014.
- [2] P. V. Lade, "Overview of constitutive models for soils, soil constitutive models: Evaluation, selection and calibration," in *Geo-Frontiers Congress*, Austin, Texas, United States, Jan. 24–26, 2005, 2005, pp. 1–34.
- [3] E. C. Leong, H. Rahardjo, and D. G. Fredlund, "A comparative study of constitutive models for unsaturated soils," in *Second Asian Conference on Saturated Soils*, Osaka, Japan, Apr. 15–17, 2003, 2003, pp. 41–46.
- [4] H. Okamura and K. Maekawa, *Nonlinear Analysis and Constitutive Models of Reinforced Concrete*. Tokyo: Gihodo, 1991.
- [5] H. Nakamura and T. Higai, "Compressive fracture energy and fracture zone length of concrete," in *ASC, Modeling of Inelastic Behavior of RC Structures Under Seismic Load*, 2001, pp. 471–487.
- [6] J. C. Lim and T. Ozbakkaloglu, "Influence of size and slenderness on compressive strain softening of confined and unconfined concrete," *J. Mater. Civil Eng.*, vol. 28, no. 2, pp. 1–7, 2016.
- [7] M. Karamloo, M. Mazloom, and G. Payganeh, "Effects of maximum aggregate size on fracture behaviors of self-compacting lightweight concrete," *Constr. Build.*, vol. 123, pp. 508–515, 2016.
- [8] A. Achouri and M. N. Amrane, "Effect of structures density and tunnel depth on the tunnel-soil-structures dynamical interaction," *Pollack Period.*, vol. 15, no. 1, pp. 91–102, 2020.
- [9] E. H. Yang and V. C. Li, "Strain-rate effects on the tensile behavior of strain-hardening cementitious composites," *Constr. Build. Mater.*, vol. 52, pp. 96–104, 2014.
- [10] D. G. Aggelis, A. C. Mpalaskas, and T. E. Matikas, "Investigation of different fracture modes in cement-based materials by acoustic emission," *Cem. Concr. Res.*, vol. 48, pp. 1–8, 2013.
- [11] J. Fiedler and T. Koudelka, "Numerical modeling of foundation slab with concentrated load," *Pollack Period.*, vol. 11, no. 3, pp. 119–129, 2016.

- [12] *ASTM D4318-00*, Standard test methods for liquid limit, plastic limit and plasticity index of soils, American Society for Testing and Materials, West Conshohocken, Pennsylvania, USA, 2010.
- [13] H. T. Hu and W. C. Schnobrich, "Constitutive modeling of concrete by using non-associated plasticity," *ASCE J. Mater. Civil Eng.*, vol. 1, no. 4, pp. 199-216, 1989.
- [14] *JSCE, No. 15*, Standard specification for concrete structures, design, Japan Society of Civil Engineers, 2007.
- [15] K. A. Tariq and T. Maki, "Mechanical behavior of cement-treated sand," *Constr. Build. Mater.*, vol. 58, pp. 54-63, 2014.
- [16] Y. Ohsaki, "Some notes on Maschke's law and non-linear response of soil deposits," *J. Fac. Eng.*, The University of Tokyo, Series B, vol. 35, no. 4, pp. 513-536, 1980.